Journal of Inclusion Phenomena and Molecular Recognition in Chemistry **10**: 471–484, 1991.

Spectral Characterization of β-Cyclodextrin : Triton X-100 Complexes

VONDA K. SMITH, THILIVHALI T. NDOU, ARSENIO MUÑOZ DE LA PEÑA†, and ISIAH M. WARNER*
Department of Chemistry, Emory University, Atlanta, Georgia 30322, U.S.A.

(Received 25 October 1990; in final form: 19 February 1991)

Abstract. The spectral characteristics of the surfactant, Triton X-100, in the absence and presence of β-cyclodextrin have been examined. The fluorescence of Triton X-100 is concentration dependent and is markedly enhanced in the presence of β-cyclodextrin. Analysis of the variations in the excitation-emission profiles of the surfactant with concentration suggests excimer emission at concentrations above the critical micelle concentration (CMC). Nuclear magnetic resonance (NMR) spectroscopy suggests that the phenyl group is included inside the CD cavity while a portion of the ethylene oxide chain extends outside the cavity. Benesi-Hildebrand type equations were derived to determine the stoichiometry and to estimate the formation constant of the CD : S_f complex.

Key words. β-cyclodextrin, Triton X-100, cyclodextrin inclusion, fluorescence spectroscopy, nuclear magnetic resonance spectroscopy.

1. Introduction

Surfactants (S_fs) are amphiphilic molecules that have the ability to self aggregate in water to form micelles above the critical micelle concentration (CMC). The micelles are formed stepwise, i.e., one monomer added at a time, such that for normal micelles, the hydrophobic tail is directed inward while the hydrophilic head is directed outward into the bulk aqueous phase. Micelles have been used as solubilizing agents and as models for hydrophobic interactions in proteins [1–5]. There are three basic categories of surfactants. Ionic S_fs are those which are either positively charged (cationic) or negatively charged (anionic). Zwitterionic S_fs have positive and negative charges, while nonionic S_fs have no charge. Nonionic surfactants have the advantage of not being complicated by the influence of the dielectric constant of the medium on the CMC, or by the influence of the solvent on the activity coefficient of the free detergent species [1].

Naturally fluorescent surfactants contain multiple-conjugated double bonds or aromatic moieties. Triton X-100 (TX-100) molecules are examples of such and contain fluorescent phenyl groups which can be used as self probes. Fluorescence spectroscopy can provide an almost ideal system of measurement because of its inherent sensitivity. An added feature of this technique is that the fluorescence intensity can be examined as a function of all useful excitation and emission

† Present address: Department of Analytical Chemistry, University of Extremadura, 06071, Badajoz, Spain.
* Author for correspondence.

wavelengths. The resulting spectra allow spectral features to be observed simultaneously as an isometric projection. This method of data representation is usually referred to as an excitation-emission matrix (EEM) [6–8].

Cyclodextrins (CDs) are composed of $\alpha(1 \rightarrow 4)$-linked glucopyranose units which form a torus shaped molecule. This structure gives CDs the ability to include guest molecules within the hydrophobic core. This inclusion is a result of interaction between the guest molecule and CD through weak van der Waals and dispersion forces [9]. Turro *et al.* [10] have reported host-guest inclusion complexes of β- and γ-CDs with a series of cationic, phosphorescent surfactant probes. The increased phosphorescence intensity, upon addition of CDs to aqueous solutions of the surfactant probes, was the result of CD-probe association. Others have also reported enhanced fluorescence for CD : S_f systems. For example, Kondo *et al.* [11] have reported pronounced fluorescence enhancement of toluidinylnaphthalene-2-sulfonate (TNS) after interaction with α-, β-, and γ-CDs. Edwards and Thomas [12] have also shown enhanced fluorescence emission of ionic surfactants with CDs. Generally, the CD cavity offers a protective microenvironment that produces enhanced excited singlet state emission. Much interest in the use of CDs is due to their ability to mimic enzymatic systems [9, 13].

A 1 : 1 stoichiometry is usually assumed for CD : S_f complexes. In some cases, a 2 : 1 stoichiometry (CD : S_f) has been reported [15–17] as well as a 1 : 2 complex (CD : S_f) [18]. It has also been noted that the reported association constants are dependent upon the concentration of S_f and the length of the hydrocarbon chain [16]. Hashimoto and Thomas [19] have provided evidence that if the hydrocarbon chain protrudes from the β-CD cavity or if the orientation of the guest molecule within the host is not thermodynamically conducive to complexation, then the formation constant will be lowered. Similarly, Satake *et al.* [20] have found that the complex stability is affected by the number of carbon atoms of the probe. As the number of carbon atoms increases, the formation constant also increases. In their studies of β-CD and anilinonaphthalenesulfonate (ANS), Catena and Bright [13] have suggested that both 1 : 1 and 2 : 1 (β-CD : ANS) complexes are formed. Both hydrogen bonding and the hydrophobic effect is usually the major factor. In this case, it can be inferred that the geometry/orientation is inherent for inclusion to occur. It should be noted that ANS is not a surfactant but is similar to TX-100 in that both contain phenyl groups and the interactions through hydrogen bonding may be similar.

A convenient means to assess the dynamic interaction of a S_f molecule with CD can be provided by NMR spectroscopy. The chemical shifts and resonance line widths of β-CD and the S_f provide effective methods for investigation of interaction sites since these parameters are sensitive to the molecular environment. Such intensities are assessed by comparing the NMR spectrum of pure CD with the spectrum of CD containing the associated molecular species. Binding may be indicated directly through changes in the widths, loss of resolution, splittings, and shifts of resonances. Henrikson [21] has reported that relatively unrestricted motion of the group containing the proton leads to slow proton relaxation and narrow NMR lines. If the molecule is restricted in the vicinity of the group containing the proton, then the relaxation rate increases and the line broadens. The associated line broadening is a result of a modification of the spin-spin relaxation time.

Nelson and Warner [22] have reported an unusual phenomenon with CD/S_f systems. Using surface tension measurements, they found that for certain S_fs, the ratio of the CMC/[CD] is constant with increasing concentration of CD. A variety of surfactants with α- and γ-CD were examined, some of which showed this trend while others did not. As a result of that initial study, a detailed examination of cyclodextrin-surfactant interactions has been initiated in this laboratory. In the studies reported here, β-CD and TX-100 interactions using spectroscopic evaluation are presented. The phenyl group of TX-100 is used as the fluorescing chromophore (see structure below). Relevant equations are derived and the resulting formation constant and stoichiometry of the system are presented as well.

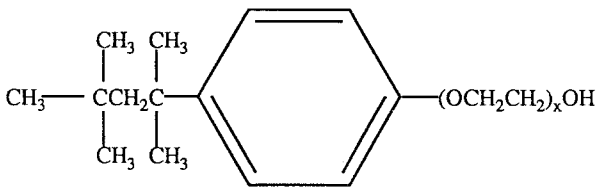

x = 9–10

2. Experimental

2.1. MATERIALS

TX-100 was obtained from Aldrich. The β-CD was obtained from American Maize Products Company (Hammond, Indiana) and was used without further purification. Deuterium oxide (Aldrich 99.9% atom D) was used as the solvent in the NMR studies.

2.2. INSTRUMENTATION

A Perkin-Elmer LS-5 fluorescence spectrophotometer has been interfaced to an IBM AT microcomputer, via an RS232 card and programmed to obtain excitation-emission matrices (EEM). The CFS v. 3.0 software program from Perkin-Elmer [23] has been modified to automatically acquire multidimensional luminescence data. This acquisition is performed by successively scanning the emission monochromator at different excitation wavelengths. The isometric projection is created using the SURFER program from Golden [24]. In the isometric projection, the spectra are displayed with the aid of a 'hidden line removal' for better visual interpretation. Contour plots are produced by connecting points of equal fluorescence using contour lines. The equifluorescence lines are calculated by linear interpolation between neighboring points in the EEM. This process locates the (λ_{ex}, λ_{em}) pair corresponding to the fluorescence of the contours. In the contour plots, the two normal axes represent the emission and excitation wavelengths, while the intensities are expressed as a series of contours. The isometric (3-D) plots were acquired by scanning the λ_{em} between 250 and 400 nm, and varying the excitation spectra in 5 nm increments from 240 to 330 nm.

Fluorescence spectra were also recorded on a Perkin-Elmer 650-10S Fluorescence Spectrophotometer equipped with a thermostatted cell housing. The excitation source was a 150 W Xenon arc lamp. Fluorescence emission spectra were taken at an excitation wavelength of 275 nm. The bandpath settings for excitation and emission slits were 5 and 3 nm, respectively. All measurements were performed in a 10 cm quartz cell at approximately 23°C. Absorbance measurements were performed on Perkin-Elmer Lambda 3C and Varian Cary 3 UV/VIS Spectrophotometers. High resolution NMR spectra were obtained using an NT-360 NB spectrometer.

2.3. METHODS

2.3.1. *TX-100 Absorbance measurements*

A 5.0×10^{-3} M stock solution of TX-100 was prepared by pipetting the appropriate volume into a 100 mL flask and diluting to the mark with deionized water. The solution was shaken using a wrist-action shaker and left standing overnight. The TX-100 samples of varying concentrations were prepared by transferring appropriate aliquots of the stock solution into 10 mL flasks and diluting to the mark with deionized water. The concentration of TX-100 ranged from 5.0×10^{-5} to 7.0×10^{-7} M. The same sample preparation method was used in all subsequent experiments.

2.3.2. *Influence of β-CD on TX-100 absorbance*

A 1.0×10^{-2} M stock solution of β-CD was prepared by transferring a weighed quantity of β-CD into a 100 mL flask and diluting to the mark with deionized water. The concentration of β-CD ranged from 0.0 to 9.0×10^{-3} M. The concentration of TX-100 was held constant at 5.0×10^{-4} M.

2.3.3. *Excitation-Emission Matrix (EEM) Studies*

The concentrations of TX-100 ranged from 5.0×10^{-6} to 7.0×10^{-4} M.

2.3.4. *TX-100 Fluorescence*

The concentrations of TX-100 ranged from 5.0×10^{-7} to 5.0×10^{-3} M.

2.3.5. *Influence of β-CD on TX-100 Fluorescence*

The β-CD concentrations ranged from 0.0 to 4.0×10^{-4} M with fixed TX-100 (5.0×10^{-6} M) concentration. In addition, 0.0 to 9.0×10^{-3} M β-CD concentrations with a fixed TX-100 (5.0×10^{-4} M) concentration were also prepared in all cases.

2.3.6. *NMR Studies*

Proton NMR spectra were recorded in D_2O at ambient temperature. The samples were equilibrated in the probe for approximately 5 minutes before each run.

Changes in the resonance line width, shifts, and intensities of the various groups in β-CD were determined from β-CD solutions containing TX-100 and compared to those taken in the absence of TX-100. Chemical shifts are expressed in ppm relative to the HOD peak.

3. Results and Discussion

3.1. TRITON X-100 UV ABSORPTION

The ultraviolet absorption spectra of aqueous TX-100 solutions show a maximum centered at 275 nm and a shoulder at around 285 nm (Figure 1a). As the concentra-

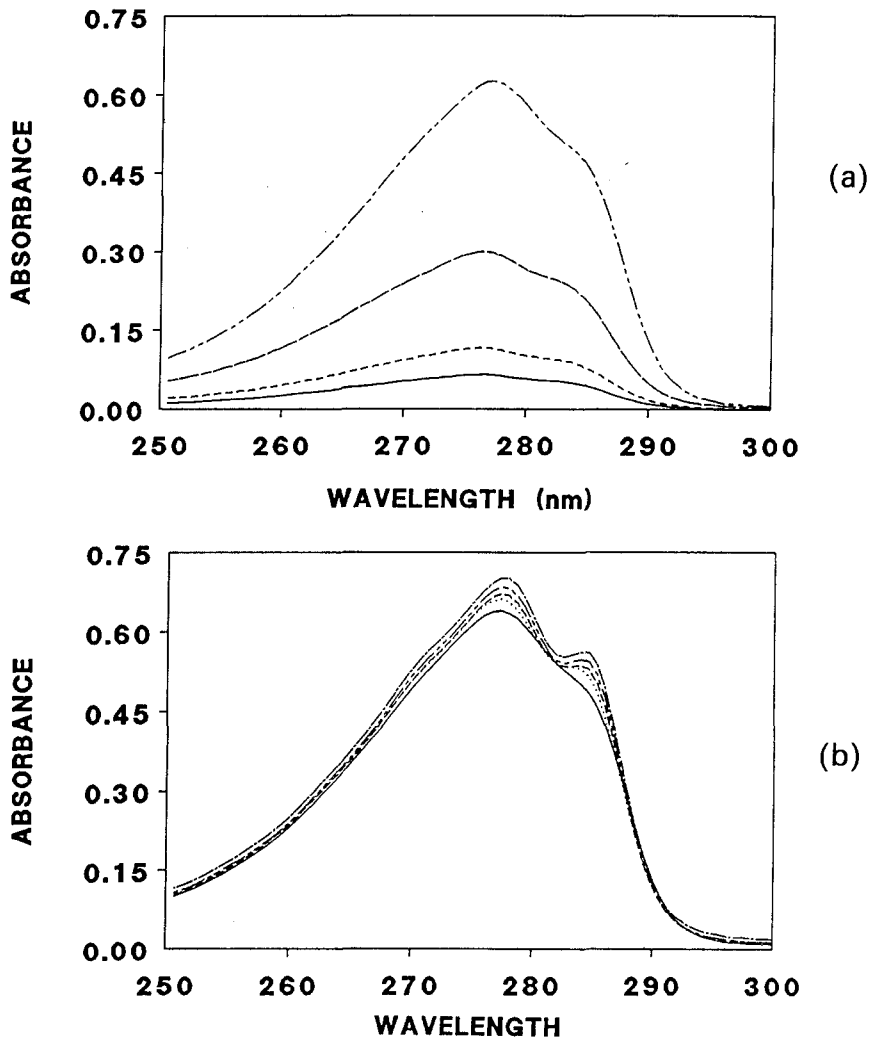

Fig. 1. (a) The effect of concentration on the absorption spectrum of Triton X-100 in water: 5.5×10^{-5} (——); 1.0×10^{-4} (- - -); 2.1×10^{-4} (– –); and 5.0×10^{-4} M (– · –). (b) Changes in the absorption spectrum of TX-100 (5.0×10^{-3} M) with increasing β-CD concentration: No CD (——); 1.0×10^{-3} (····); 2.0×10^{-3} (- - -); 3.0×10^{-3} (– · –); and 4.0×10^{-3} M (–·–) β-CD.

tion of TX-100 is increased from below the CMC to above the CMC, the absorbance increases and is accompanied by a 2 nm red shift at concentrations above the CMC. This is in agreement with the observations of Gratzer and Beaven [1] and Ray and Némethy [2] who reported changes in the vibrational structure, molar absorptivity and a concomitant red shift of TX-100 as the concentration is increased.

To clarify the role of micelles in fluorescence emission, especially in the case where the micelle itself is the probe, it is important to independently determine the CMC. The CMC can be determined from a plot of molar absorptivity vs concentration of surfactant [25]. In this study, a CMC value of about 2.7×10^{-4} M was determined for the system using this method.

3.2. β-CD/TX-100 UV ABSORBANCE

The absorbance spectra for aqueous β-CD/TX-100 solutions are shown in Figure 1b. The absorbance of TX-100 increases until 4.0×10^{-3} M β-CD and remains relatively constant as higher concentrations are added. The spectral band becomes narrower and the shoulder that is poorly defined in the absence of β-CD is more distinct. The absorbance shows a 2 nm red shift when the β-CD concentration in a 5.0×10^{-4} M TX-100 is brought to 4.0×10^{-3} M. This shift is consistent with the observations of Crooks [26] who reported that the effect is due to an auxochrome, an electron donating component that is non absorbing. Such components have the ability to modify the absorption of molecules containing chromophores. In this case, this suggests that the interaction between the phenyl moiety of TX-100 and the electron donating hydroxyl and glycosidic oxygens of β-CD are likely responsible for the bathochromic shift. The ratio of peak maxima increases upon the initial addition of β-CD, then remains relatively constant at higher CD concentrations.

3.3. TRITON X-100 EEM

Figure 2a shows the contour plot of a 5.0×10^{-6} M solution of TX-100. The plot shows a peak at $\lambda_{ex} \approx 275$ nm and $\lambda_{em} \approx 305$ nm. The large ridge that appears diagonally across the spectrum with peak maxima at $\lambda_{ex} = \lambda_{em}$ is attributed to first-order scattering. Fluorescence spectra show Raman bands at low TX-100 concentrations and are located near the Rayleigh scatter. In Figure 2a, the Raman bands are not very distinguishable due to the large first order scattering ridge. Higher concentrations show similar features, but a new spectral band appears at $\lambda_{ex} \approx 275$ nm and $\lambda_{em} \approx 330$ nm at concentrations above the CMC. For concentrations well above the CMC (3.0×10^{-3} M), the EEM also shows a dramatic difference in the corrected excitation spectrum (Figure 2b). There appears to be two excitation maxima centered at 285 and 252 nm (Figure 2c).

A single emission peak is observed below the CMC, and two above the CMC. The excitation spectrum also shows significant changes which are concentration dependent. There is a single excitation peak at concentrations below the CMC and two at concentrations well above the CMC. This suggests that the new spectral band appearing around 330 nm is due to dimer or excimer emission at concentrations above the CMC.

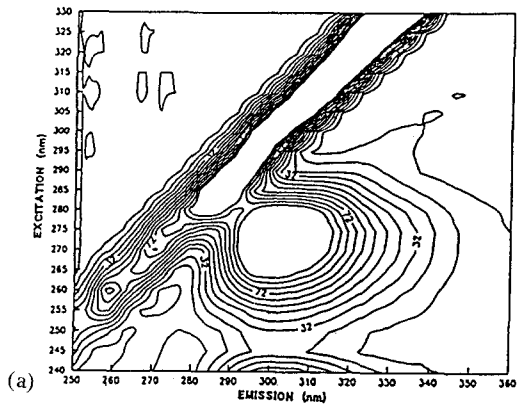

(a)

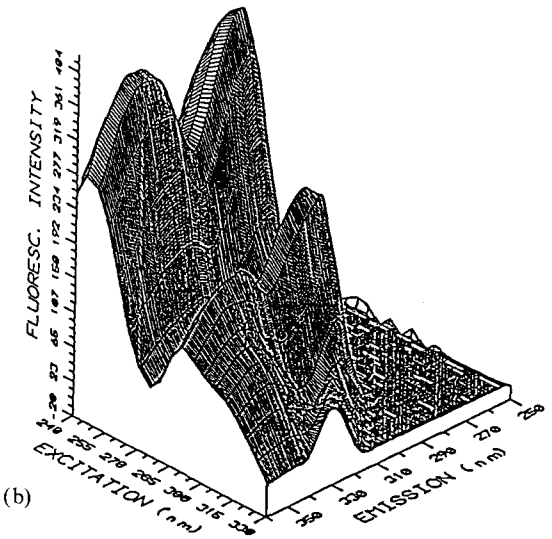

(b)

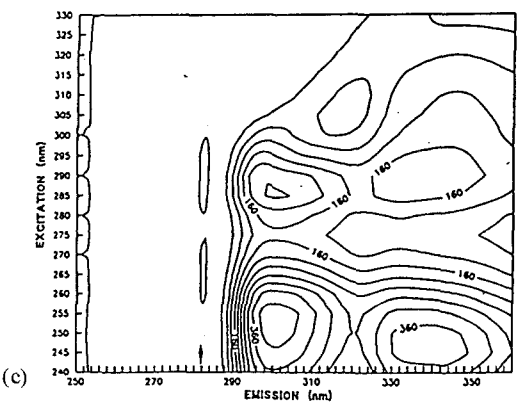

(c)

Fig. 2. EEM spectra of Triton X-100: (a) Contour plot of 5.0×10^{-6} M TX-100 (below the CMC) (b) 3-D spectrum of 3.0×10^{-3} M TX-100 (above the CMC) (c) Contour plot at the same concentration.

3.4. TRITON X-100 FLUORESCENCE

The fluorescence emission spectra of TX-100 is shown in Figure 3. At concentrations below the CMC, the spectrum shows a large peak centered around 305 nm. Additional bands appear at concentrations above the CMC, with the maxima at 330 and 348 nm. Kalyanasundaram and Thomas [25] have attributed similar spectral bands to dimeric species that appear at higher concentrations. This is also consistent with the results reported by Ndou and von Wandruszka [27] using benzalkonium chloride surfactants. They rationalized this effect in terms of the mutual proximity of the phenyl groups in the micelles giving rise to the excimer band. In this work, the appearance of the new bands is accompanied by a change in the shape of the band at 305 nm. It becomes less broad and the maximum appears to blue shift by approximately 3 nm.

3.5. EFFECT OF β-CD CONCENTRATION

Figure 4 shows the increase in relative fluorescence intensity with increasing β-CD concentration. The intensity was measured at the maximum TX-100 peak of 305 nm, resulting from the monomer emission. The TX-100 fluorescence intensity increases sharply at low concentrations of β-CD and then reaches a constant level around 3.0×10^{-3} M β-CD. This may indicate that the monomeric units have, essentially, been included within the β-CD cavity. Addition of β-CD to TX-100 solutions at concentration above the CMC results in the disappearance of the excimer band. This suggests the deaggregation of TX-100 dimers and the concomitant multimers, when the β-CD concentration is increased. This appears true at a constant TX-100 concentration well below the CMC and excess β-CD. For systems such as these, there is competition between TX-100 micelles and β-CD for the monomeric units. However, at concentrations below the CMC, no competition is expected from the micelles since they should not exist at these concentrations.

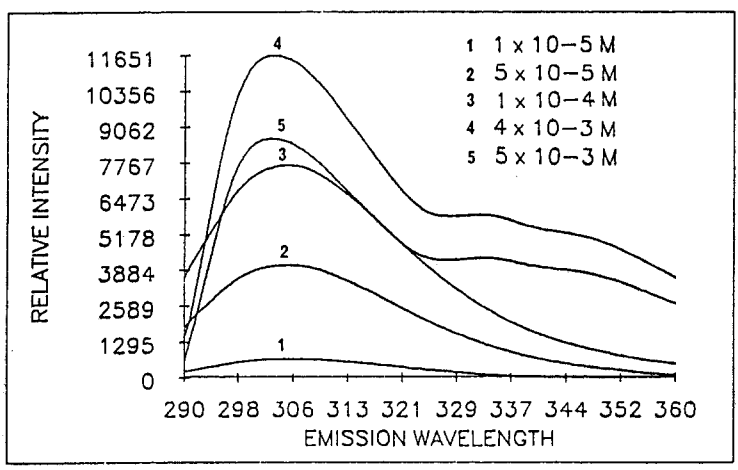

Fig. 3. Fluorescence emission spectra of TX-100 at various concentrations.

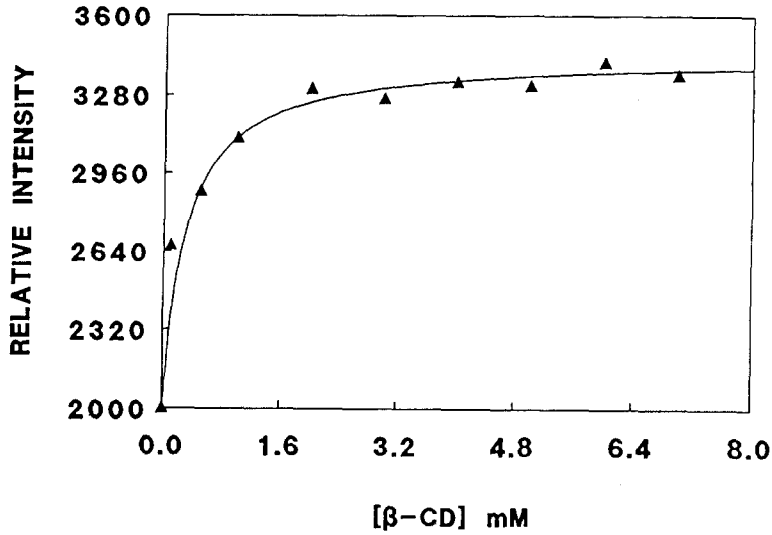

Fig. 4. Relative fluorescence intensity of TX-100 at different concentrations of β-CD. Conditions: $\lambda_{ex} = 275$ nm, $\lambda_{em} = 305$ nm, [TX-100] = 5.0×10^{-6} M.

3.6. NMR OF THE β-CD/TX-100 SYSTEMS

It is well established that nonionic surfactants consist of two distinct regions: a non-polar, dry core, made up of aliphatic and/or aromatic moieties, and a relatively wet outer sheath [14, 28]. In the case of TX-100, the outer sheath consists of partially hydrated polar oxide units. The NMR spectrum of micellized TX-100 is shown in Figure 5a. The spectrum consists of peaks from six kinds of protons: the terminal methyl singlet (a-CH_3, at δ 0.67), the internal methyl singlet (c-CH_3, at δ 1.26), the methylene singlet (b-CH_2, at δ 1.64) and the phenyl ring proton singlets (d-H_2 and e-H_2 at δ 6.89 and 7.21 respectively). The ethylene oxide (EO) proton resonances result in a large and unresolvable, broad peak at around 3.65 ppm. Podo *et al.* [29] have shown similar proton NMR spectra using *p*-tertoctylphenoxy(polyoxy)ethanol surfactants. The broadness of the EO peak was attributed to changes in the local microenvironment due to contact with water at the first of the ethoxy units adjacent to the phenyl group. Figure 5b is the NMR spectrum of pure β-CD consisting of peaks from five kinds of protons: the H-1 doublet [at δ 5.06 (this region is not included in the figure)], the H-3 triplet (at δ 3.96), a strong, unresolved broad peak consisting of H-6 and H-5 (at δ 3.87–3.85), the H-2 appearing as two doublets (at δ 3.64), and the H-4 triplet (at δ 3.58).

The addition of β-CD to the TX-100 solution causes a split of some of the TX-100 resonance lines. The degree of splitting is different for protons at different positions in the TX-100 molecule. The c-CH_3 resonance line is split into two peaks of comparable size (Figure 5c). The geminal methylene protons (b-CH_2) show an AB type splitting, giving a quartet. The most notable changes occur in the phenyl ring proton resonances; these are split into two well resolved peaks. The β-CD dramatically hinders the high rotational freedom of the b-CH_2, c-CH_3, d-H_2, and e-H_2 protons. This strongly suggests different mobilities of the protons contributing

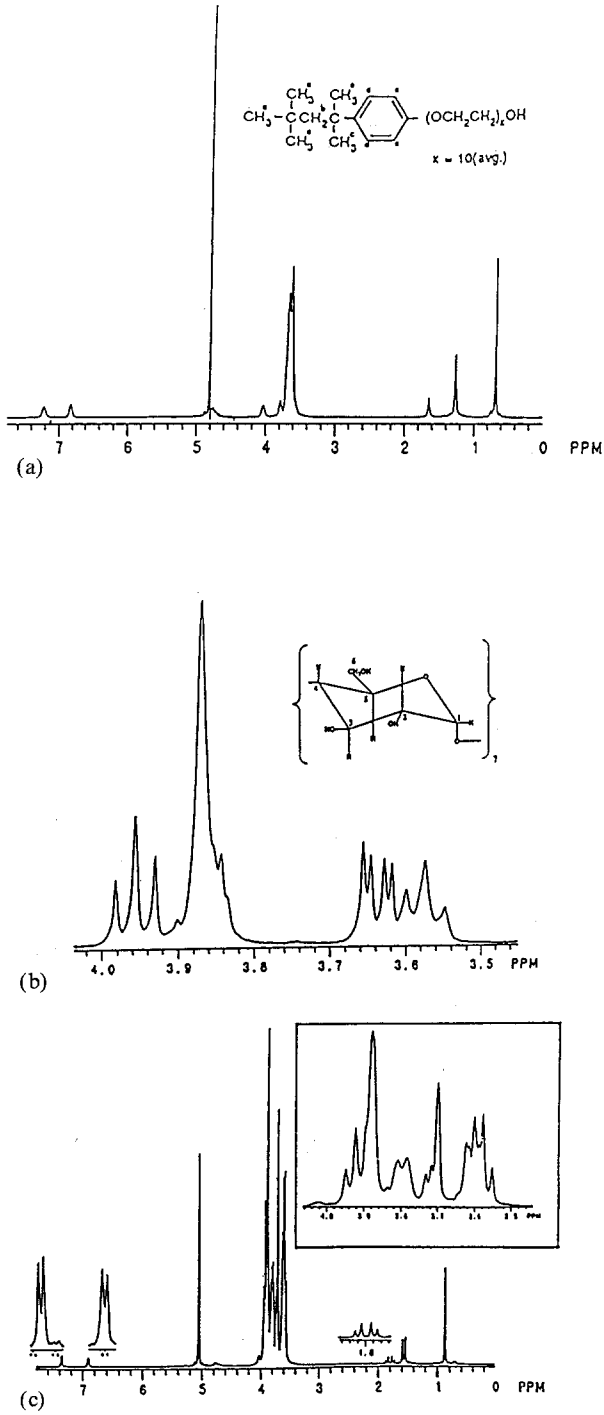

Fig. 5. Proton NMR spectra in D_2O of (a) 1.0×10^{-3} M TX-100 (b) 5.0×10^{-3} M β-CD (c) β-CD solution containing TX-100.

to the singlet bands. The groups/protons no longer experience identical chemical environments, and therefore show different chemical shifts. The mobility of this dry portion of the hydrocarbon chain is rather restricted and consequently, different splitting is observed.

A slight upfield shift (0.03 ppm) of the H-3 signal [Figure 5c (inset)] of β-CD is observed in the presence of TX-100. Furthermore, the signals between 3.70–3.85 ppm are likely due to the H-5 proton shifting upfield from the region where H-5 and H-6 appear in the pure β-CD spectrum. The assignments of these shifted signals to H-5 is because H-3 and H-5 are located inside the CD cavity. It is likely that both the H-3 and H-5 protons would shift in the same way, providing a rationale for these assignments. The spectral features observed suggest a strong interaction between TX-100 and the H-3 and H-5 protons in the interior of the β-CD cavity. Similar observations were reported by Turro *et al.* [10] who noted upfield shifts of the H-5 protons of β-CD in the presence of [5-(4-bromo-1-naphthoyl)pentyl]tri-methylammonium bromide. The association between β-CD and TX-100 appears to take place through the phenyl ring and part of the hydrocarbon chain (c-CH_3 and b-CH_2) as indicated by changes in the NMR resonances of these groups. Some line broadening of the EO peak is attributable to those groups (—OCH_2CH_2—) in the chain that are located adjacent to the phenyl ring. This suggests that the presence of β-CD slows the proton exchange and thus new resonances are observed with different appropriate multiplets. Therefore, it could be inferred that part of the TX-100 molecule is included inside the β-CD cavity. The a-CH_3 proton signals remain unaffected, suggesting a free rotation, and that these groups are not involved in interaction inside the β-CD cavity.

It is interesting to note the distinct changes occurring at the H-2 and H-4 resonances after addition of TX-100 to the β-CD solution. These protons are located on the exterior of the β-CD torus, and the dramatic loss in resolution of these signals is likely due to interaction with the EO groups of TX-100. Clearly, the association between β-CD and TX-100 is such that the mutual orientation of the ethylene oxides result in a strong interaction with the protons at the exterior of the CD torus.

3.7. ASSOCIATION CONSTANT OF β-CD : TX-100 COMPLEX

The relative fluorescence intensity of TX-100 increases in the presence of β-CD as is shown in Figure 4 (see Section 3.5). The emission enhancement phenomenon is used here to determine the stoichiometry and the formation constant of the β-CD : TX-100 complex as follows. Assuming that β-CD forms a 1 : 1 inclusion complex with TX-100 as shown below,

$$CD + S_f \rightleftharpoons CD : S_f, \tag{1}$$

the formation constant of the complex (K_1) is defined by

$$K_1 = \frac{[CD : S_f]}{[CD][S_f]} \tag{2}$$

where [CD], [S_f], and [CD : S_f] are the equilibrium concentrations of CD, S_f and the complex, respectively. When the initial concentration of CD ([CD]$_0$) is in large

excess compared to the concentration of the complex, the following simplification can be applied: $[CD] = [CD]_0 - [CD : S_f] \approx [CD]_0$ because $[CD]_0 >>> [CD : S_f]$. Thus, from mass balance, we have

$$[S_f]_0 = [S_f] + [CD : S_f] \tag{3}$$

where $[S_f]_0$ is the initial concentration of TX-100. Consequently, Equation 2 can be simplified as follows:

$$K_1 = \frac{[CD : S_f]}{[CD]_0([S_f]_0 - [CD : S_f])}. \tag{4}$$

As β-CD is not fluorescent, the observed fluorescence intensity is the sum of the contributions from free and complexed TX-100, which can be represented by the following expression:

$$F = k_s[S_f] + k_c[CD : S_f] \tag{5}$$

where k_s and k_c denote the proportionality constants relating the intensities and concentrations of the S_f and $CD : S_f$ species, respectively. The fluorescence intensity of TX-100 in the absence of β-CD is represented by:

$$F_0 = k_s[S_f]_0. \tag{6}$$

For a sufficiently high CD concentration, all of the TX-100 molecules are complexed with β-CD and the fluorescence intensity is represented by

$$F_\infty = k_c[CD : S_f]. \tag{7}$$

Under these conditions, $[S_f] = 0$ and $F_\infty = k_c[S_f]_0 = \text{constant}$. Thus, the fraction of TX-100 complexed is given by the following equation:

$$\frac{[CD : S_f]}{[S_f]_0} = \frac{F - F_0}{F_\infty - F_0}. \tag{8}$$

Combining Equations (4) and (8) and rearranging, we arrive at

$$\frac{F - F_0}{F_\infty - F_0} = \frac{K_1[CD]_0}{1 + K_1[CD]_0}. \tag{9}$$

Equation (9) can be simplified as follows:

$$\frac{F - F_0}{[CD]_0} = (F_\infty - F_0)K_1 - (F - F_0)K_1. \tag{10}$$

Thus, a plot based on Equation 10 may be used to determine the stoichiometry of this complexation. If the assumption of a 1 : 1 stoichiometry for the complex is applied, plotting $(F - F_0)/[CD]_0$ vs $(F - F_0)$ should give a straight line, and K_1 can be estimated from the slope. A linear relationship is obtained for this system with our data.

The linear relationship obtained, allows us to conclude a 1 : 1 stoichiometry for the β-CD : TX-100 complex. (It should be noted that when the data is fitted for a 2 : 1 β-CD : TX-100 complex, a curvilinear relationship is obtained, suggesting that the stoichiometry of the complex is not 2 : 1). However, the linear transformation that is used here does not properly weight these data [30]. A better estimation of K_1

is obtained by nonlinear regression analysis (NLR) [31]. The direct relationship between the observed fluorescence intensity, F, and the β-CD concentration, $[CD]_0$, is given by

$$F = F_0 + \frac{(F_\infty - F_0)K_1[CD]_0}{1 + K_1[CD]_0}. \tag{11}$$

By using this equation, the experimental data can be directly fitted. The initial parameter estimates needed for the nonlinear regression method have been obtained from the linear plots. The calculated association constant is $K_1 = 3327\ M^{-1}$.

4. Conclusions

The association of TX-100 molecules with CD, results in a marked increase in fluorescence intensity of the phenyl moiety of the surfactant. This increase indicates a change in the microenvironment of the phenyl groups of TX-100. This microenvironmental change infers a change in the hydrophobicity, likely caused by inclusion of TX-100 within the hydrophobic β-CD cavities. In addition, the fluorescence intensity reaches a maximum with increasing β-CD concentration, suggesting that the complexation reaction between TX-100 and β-CD has reached completion.

The calculated formation constant of $3327\ M^{-1}$ is large compared to that reported by Nelson and Warner [22] for β-CD and Igepal CA520 of $1850\ M^{-1}$ which was determined from surface tension data. Igepal CA520 differs in structure from TX-100 only in the EO chain length. This formation constant is also rather large when compared with those previously reported between β-CD and sodium salts of n-alkane sulfonates (C_nS) and n-alkyl sulfates (C_nOS) [15]. The low formation constants obtained in these studies were likely due to the competitive inhibition of association of the S_fs by the ANS probes. A low formation constant ($590\ M^{-1}$) was reported for γ-CD and [10-(4-bromo-1-naphthoyl)decyl]trimethylammonium bromide ($BNK\text{-}10^+$) by Turro *et al.* [10]. The complexation process was rationalized in terms of the way the $BNK\text{-}10^+$ molecule positioned itself in a folded manner inside the larger cavity diameter of γ-CD. On the basis of molecular size, it is apparent that the phenyl ring of TX-100 ($\sim$3.0 Å wide and 5.0 Å long) is small such that it completely fits inside the β-CD cavity (inner diameter of 7.8 Å wide and a length of 7.8 Å). The large diameter of the β-CD cavity may allow more of the hydrocarbon chain to be included inside the CD. In view of our findings, the most plausible explanation of the orientation of the surfactant inside the β-CD cavity resembles that of Turro, showing the S_f coiled inside the cavity. This is consistent with the NMR results which show that part of the hydrocarbon chain, phenyl group, and probably part of the EO chain adjacent to the phenyl group come into close proximity with the H-3 and H-5 protons of the β-CD.

Acknowledgements

The authors acknowledge the National Science Foundation (CHE-9001412) for support of this work and an NSF instrumentation grant (CHE-8206103) for use of an NT-360 NB NMR spectrometer. A.M.P. acknowledges support from D.G.I.C.Y.T. of the Ministry of Education and Science of Spain for the grant that

made possible his research in Professor Warner's laboratory. The authors are grateful to G. A. Reed of American Maize Products for providing the CDs used in this study and Karen L. Greene for her help with obtaining the NMR data.

References

1. W. B. Gratzer and G. H. Beaven: *J. Phys. Chem.* **73**, 1 (1969).
2. A. Ray and G. Némethy: *J. Phys. Chem.* **75**, 804 (1971).
3. P. M. Torgerson, H. G. Drickamer, and G. Weber: *Biochemistry* **18**, 3079 (1979).
4. S. Razin: *Biochem. Biophys. Acta* **265**, 241 (1972).
5. E. A. Dennis: *J. Supramol. Struct.* **2**, 682 (1974).
6. G. Weber: *Nature* **190**, 27 (1961).
7. I. M. Warner, J. B. Callis, E. R. Davidson, and G. D. Christian: *Anal. Lett.* **8**, 655 (1975).
8. I. M. Warner, G. D. Christian, E. R. Davidson, and J. B. Callis: *Anal. Chem.* **49**, 564 (1977).
9. W. Saenger: *Angew. Chem. Int. Ed. Engl.* **19**, 344 (1980).
10. N. J. Turro, T. Okubo, and C-J. Chung: *J. Am. Chem. Soc.* **104**, 1789 (1982).
11. H. Kondo, H. Nakatani, and K. Hiromi: *J. Biochem.* **79**, 393 (1976).
12. H. E. Edwards and J. K. Thomas: *Carbohydr. Res.* **65**, 173 (1978).
13. G. C. Catena and F. V. Bright: *Anal. Chem.* **61**, 905 (1989).
14. N. J. Turro and P. C. Kuo: *Langmuir* **1**, 170 (1985).
15. J. W. Park and H. J. Song: *J. Phys. Chem.* **93**, 6454 (1989).
16. R. Palepu and V. C. Reinsborough: *Can. J. Chem.* **66**, 325 (1988).
17. A. Hersey, B. H. Robinson, and H. C. Kelly: *J. Chem. Soc. Faraday Trans. I* **82**, 1271 (1986).
18. J. Szejtli: *Cyclodextrins and Their Inclusion Complexes*, Akademiai Kiado, Budapest (1982).
19. S. Hashimoto and J. K. Thomas: *J. Am. Chem. Soc.* **107**, 4655 (1985).
20. I. Satake, T. Ikenoue, T. Takeshita, K. Hayakawa, and T. Maeda: *Bull. Chem. Soc. Jpn.* **58**, 2746 (1985).
21. K. P. Henrikson: *Biochem. Biophys. Acta* **203**, 288 (1970).
22. G. Nelson and I. M. Warner: *Carbohydr. Res.* **192**, 305 (1989).
23. *Perkin-Elmer Fluorescence Applications Program for LS-3b, -4, -5b Fluorescence Spectrometers*, CFS version 3.0, 1988.
24. Golden Software, Inc. P.O. Box 28, Golden, Colorado 80402.
25. K. Kalyanasundaram and J. K. Thomas: *Micellization, Solubilization, and Microemulsions* (Ed. K. L. Mittal), Vol. 2, Plenum Press, N.Y. (1977).
26. J. E. Crooks: *The Spectrum in Chemistry*, Academic Press, London, England; New York, N.Y. (1978).
27. T. T. Ndou and R. von Wandruszka: *Talanta* **36**, 485 (1989).
28. W. J. Dressick, B. L. Hauenstein, T. B. Gilbert, J. N. Demas, and B. J. DeGraff: *J. Phys. Chem.* **88**, 3337 (1984).
29. F. Podo, A. Ray, and S. Némethy: *J. Am. Chem. Soc.* **95**, 6164 (1973).
30. K. A. Connors: *Binding Constants. The Measurement of Molecular Complex Stability*, John Wiley and Sons, N.Y. (1987).
31. SAS/STAT, Release 6.03, Cary, NC: SAS Institute.